Fermi National Accelerator Laboratory

FERMILAB-TM-2045

CDF Forward Shielding for Run II

O.E. Krivosheev and N.V. Mokhov

Fermi National Accelerator Laboratory
P.O. Box 500, Batavia, Illinois 60510

March 1998

Operated by Universities Research Association Inc. under Contract No. DE-AC02-76CH03000 with the United States Department of Energy

Disclaimer

This report was prepared as an account of work sponsored by an agency of the United States Government. Neither the United States Government nor any agency thereof, nor any of their employees, makes any warranty, expressed or implied, or assumes any legal liability or responsibility for the accuracy, completeness, or usefulness of any information, apparatus, product, or process disclosed, or represents that its use would not infringe privately owned rights. Reference herein to any specific commercial product, process, or service by trade name, trademark, manufacturer, or otherwise, does not necessarily constitute or imply its endorsement, recommendation, or favoring by the United States Government or any agency thereof. The views and opinions of authors expressed herein do not necessarily state or reflect those of the United States Government or any agency thereof.

Distribution

Approved for public release; further dissemination unlimited.

CDF Forward Shielding for Run II

O. E. Krivosheev and N. V. Mokhov

March 16, 1998

Fermi National Accelerator Laboratory
P.O. Box 500, Batavia, Illinois 60510

Abstract

Detailed calculations of the accelerator related background in the CDF forward muon spectrometer have been performed with the MARS13 code and a newly developed C++ code for particle tracking in accelerator lattices. Calculated space distributions of background hits are in a good agreement with data taken in Run I. Several shielding configurations in the CDF hall and Tevatron tunnel have been studied. The optimal one provides a 30-fold shielding efficiency compatible with CDF Run II requirements.

1 Introduction

The CDF detector [1] performance at the increased luminosity of Run II will strongly depend on background hit rates in detector components [3]. In addition to severe radiation from the $p\overline{p}$ interaction point (IP), CDF, as any other collider detector, is exposed to particle fluxes from the accelerator tunnel [3, 4]. Without protection, the number of hits from halo particles in the detector can be equal to or even greater than the number of hits from particles originating from the IP and their products [5]. Reduction of beam loss rate in the interaction region and plugging the accelerator tunnel at the entrance to the experimental hall are the ways to improve the situation. A full calculation study, design and installation of the shielding walls at both ends of the DØ detector hall were done at the Tevatron [6] resulting in almost a 10-fold suppression of the accelerator backgrounds. The work is underway to re-design the forward regions of both the DØ and CDF detectors to meet the Run II era. This paper describes studies towards the CDF upgrade.

2 Calculation Model

Realistic Monte Carlo simulations of accelerator background formation in the CDF detector (Fig. 1) are done in two stages. At the first stage, beam loss distributions in

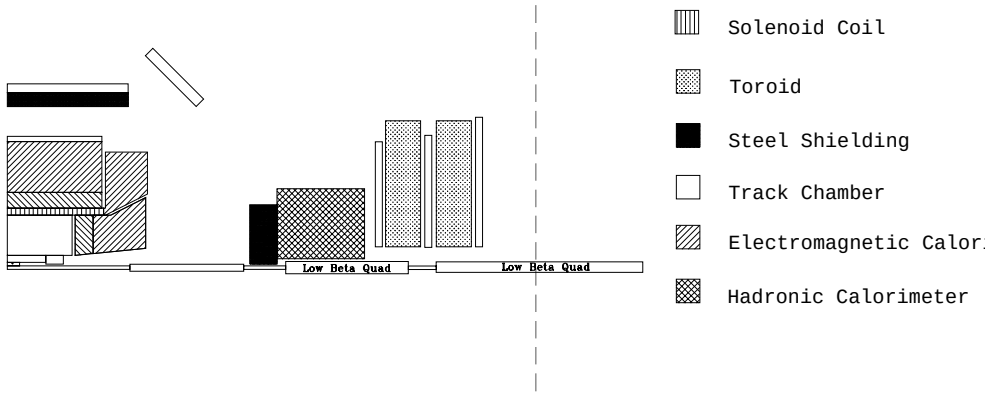

Figure 1: The CDF detector Run I layout

Tevatron are calculated in this study with a newly developed code, STRUCT++, via tracking protons through the Tevatron lattice and recording the particles lost in the BØ vicinity. The code inherits main features of the STRUCT code [7] and uses the physics modules of the MARS13 code system [8]. C++ versions of MARS13 subroutines are used to simulate proton-nucleus inelastic and elastic interactions, multiple Coulomb scattering and energy loss with straggling with special algorithms to ensure a proper edge-scattering treatment. The C++ library developed at Fermilab [9, 10] was adapted to accommodate the Tevatron aperture and geometry restrictions. The ability to store complete information on lost protons is provided for each beam element. Calculated longitudinal distributions of energy deposition and charged hadron flux (E>0.5 GeV) in the BØ interaction region steel beam pipe (with inner and outer radii of 3.5 cm and 3.62 cm, respectively) are shown in Fig. 2.

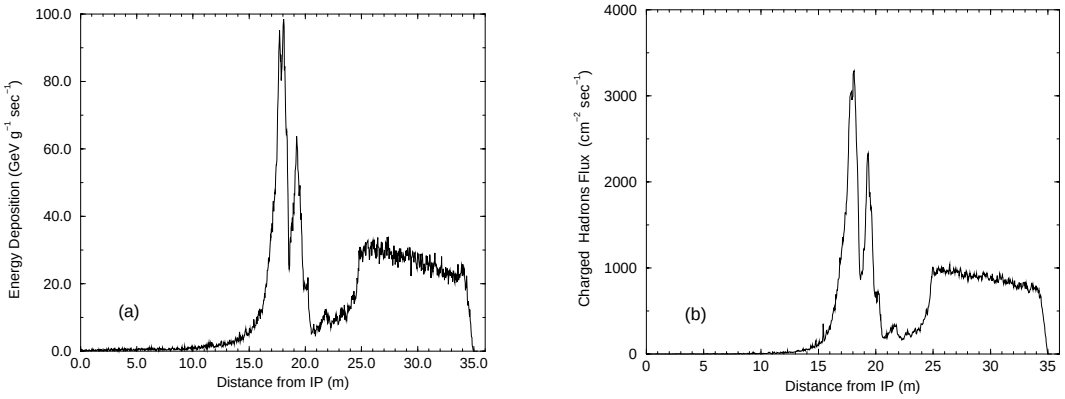

Figure 2: Beam loss source term in the BØ beam pipe: (a) energy deposition density; (b) high energy hadron flux.

At the second stage, beam loss induced hadronic and electromagnetic showers with muon production are simulated with the MARS13 code [8]. In this study a detailed description of geometry, materials and magnetic fields is taken into account for CDF near-beam components, all forward detectors, experimental hall, tunnel, shielding and Tevatron optic elements in the $\pm$36-m region from BØ .

To compare to Run I data on hit distributions in the CDF forward muon spectrometer, the calculated hit rate integrated over the muon rear plane is normalized to the appropriate experimental value: calculated energy deposition density (GeV $g^{-1}s^{-1}$) is multiplied by K_{ed}=766.18, and charged particle flux ($cm^{-2}s^{-1}$) is multiplied by K_F=2.45. These normalization convention and constants are used throughout the rest of the report.

3 Run I

In Run I, the forward muon planes were located at 9.8 m (*front*), 11.4 m (*middle*) and 13.0 m (*rear*) from IP with hadronic calorimeter as shown in Fig. 1. The baseline 1.8 m thick concrete wall (Wall-1) is installed in the tunnel at 18 m from IP. The muon chambers are made of four layers of copper clad G-10 3 mm thick. The gaps between the layers are 22 mm thick and the wires are 63-μm stainless steel. The particle passing through the chamber sees 3 mm G-10, 22 mm of argon-ethane mixture, 6 mm G-10, 22 mm argon-ethane mixture, and 3 mm G-10. The drift cell walls are 1 mm aluminum spacers parallel to the sense wires. The chamber frames are solid G-10. The toroid field at 600 amp is 1.8 T at 120-cm radius and 1.6 T at 300 cm. For both East and West toroids, the current in the coils when viewed from IP flows radially inward, which focuses μ^+. The magnetic field at the top of the West toroids pointed North. In addition to the *front*, *middle* and *rear* chambers, there are also *front* and *rear* scintillator planes. The scintillator nearer to IP on the *front* and farther from IP on the *rear* are separated from the chambers by about 5 cm.

Experimental data from CDF Run 76266 [2] were obtained with antiprotons cogged away by 1.75 μsec outside the drift window of the muon chambers. Total number of hits were collected in the five radial and eight azimuthal bins. Radial

Table 1: Radial bins in the CDF muon planes.

Radial Bin Number	Front	Middle	Rear
1	48.0-98.0	54.0-110.0	64.0-129.8
2	98.0-132.0	110.0-154.0	129.8-175.5
3	132.0-179.0	154.0-209.0	175.5-237.8
4	179.0-244.0	209.0-283.0	237.8-323.2
5	244.0-300.0	283.0-349.0	323.2-397.4

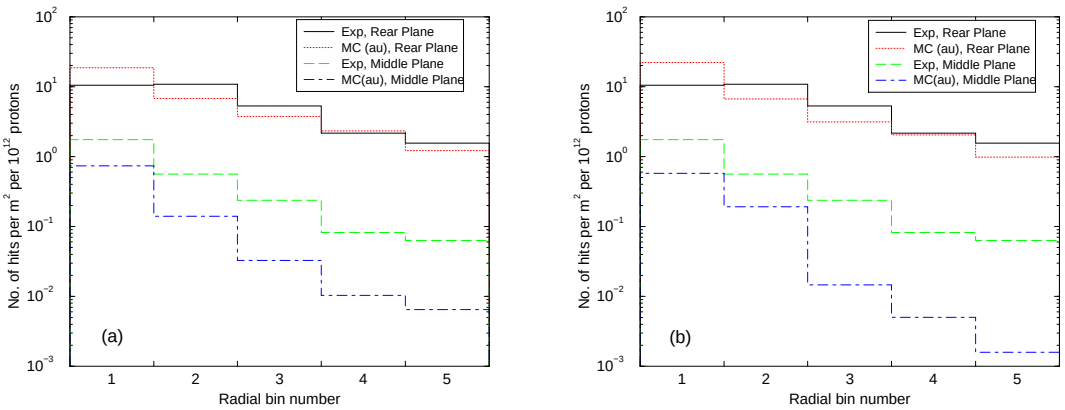

Figure 3: Calculated and measured radial distributions of azimuthally averaged hits in rear and middle planes (Run I): (a) energy deposition based calculations; (b) charged particles flux based calculations.

bin subdivision is shown in Table 1 for muon planes. Eight azimuthal bins represent equal subdivision of 360°, i.e. each bin is a 45° sector. Zero azimuthal point is located at nine o'clock from proton's eye view. Total number of hits collected are normalized to hits per m^2 per 10^{12} circulating protons.

In all cases hit rates are presented as based both on the calculated energy deposition density in the detector elements and flux of charged particles in the same radial and azimuthal bins. Calculated and measured in Run I radial distributions of azimuthally averaged hits in rear and middle planes are presented in Fig. 3. There is a very good agreement between calculations and data for the rear plane and, as expected, calculated hit rate is underestimated (low statistics in Monte Carlo) in the middle plane which is well protected by a bulk toroid material. Calculated azimuthal

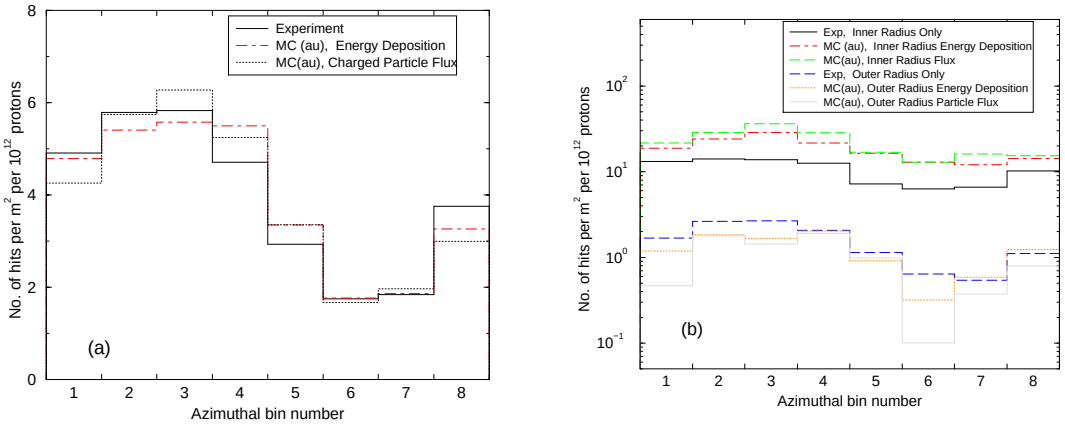

Figure 4: Calculated and measured azimuthal distributions of hits in the rear plane (Run I): (a) radially integrated; (b) inner and outer radial bins.

distributions agree also very well with data (Fig. 4), reproducing peaks and dips arising from the configuration asymmetry and effect of magnetic field.

Calculated and normalized as described in the previous section total number of hits in the rear plane is 3.94. In the middle plane, one gets 0.082 (based on energy deposition) and 0.068 (based on charged particle flux).

4 Run II

In Run II, the muon system is moved closer to IP by 4.7 m and recycled hadronic calorimeter can be used as shielding in the experimental hall. Six shielding configurations (Fig. 5) have been explored in this study:

1. A recycled hadronic calorimeter at 11 m from IP (27 layers of 2-in steel and 1-in gaps filled with poly).
2. The same recycled calorimeter at 12.8 m from IP.
3. A DØ -like collar shielding with 40 cm of steel followed by 10 cm of poly with 4 cm of lead radially in the 11-17.75 m region.
4. The same collar shielding as in configuration-3, but with an additional 1.8-m thick concrete wall at the hall/tunnel interface (Wall-2), with a 30-cm gap filled with polyethylene.
5. The same as configuration-4, but without Wall-1 in the tunnel.
6. The same as configuration-5, but additionally with the recycled calorimeter as in configuration-2.

The Run I normalization convention and constants are used for Run II case. Fig. 6 shows azimuthally averaged radial distributions of hit rates in the rear plane for the baseline and for the six considered shielding configurations. Corresponding azimuthal distributions of radially integrated hits are presented in Fig. 7. One sees that the configurations 3 to 6 give significant reduction in the number of hits. In the baseline configuration, the total number of hits (energy deposition based) in the rear plane is 1.77. Respectively, results for the considered shielding configurations are given in the second column of Table 2 and the shielding efficiencies (background reduction factor) – in the third column. Remarkably good background suppression of a factor of $\sim$30 is achieved for the fourth configuration, where the new 1.8-m wall (Wall-2) traps nicely the radiation from the tunnel. The configurations 5 and 6 do also rather well.

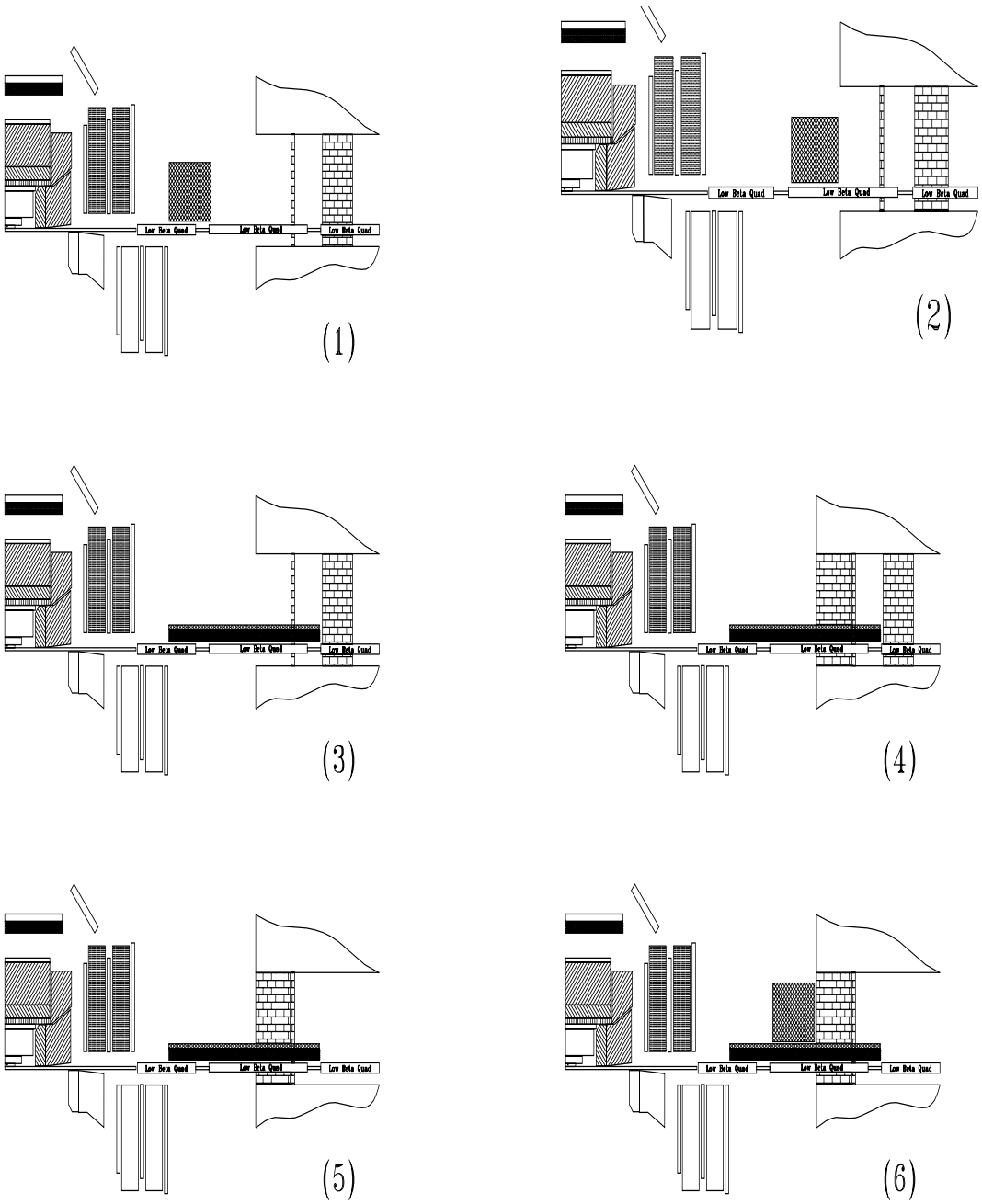

Figure 5: The CDF studied shielding configurations.

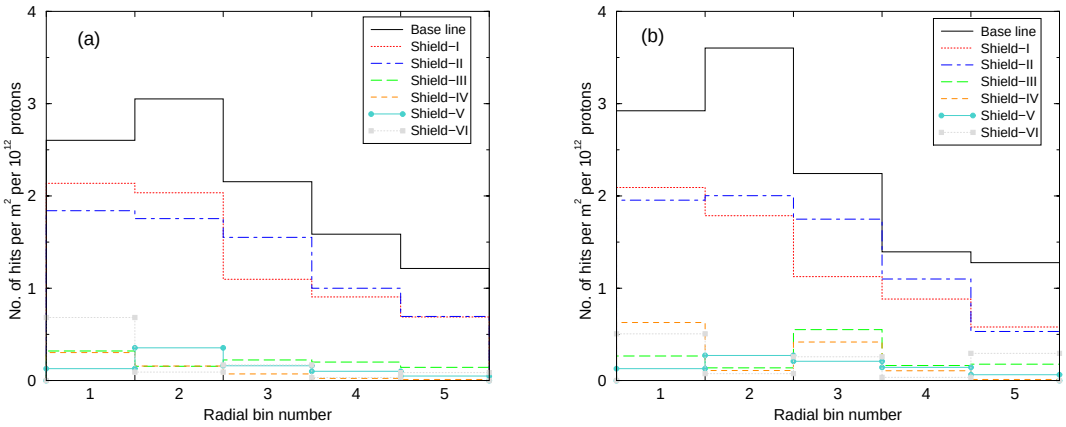

Figure 6: Radial distributions of azimuthally averaged hits in the rear plane (Run II): (a) energy deposition based calculations; (b) charged particles flux based calculations.

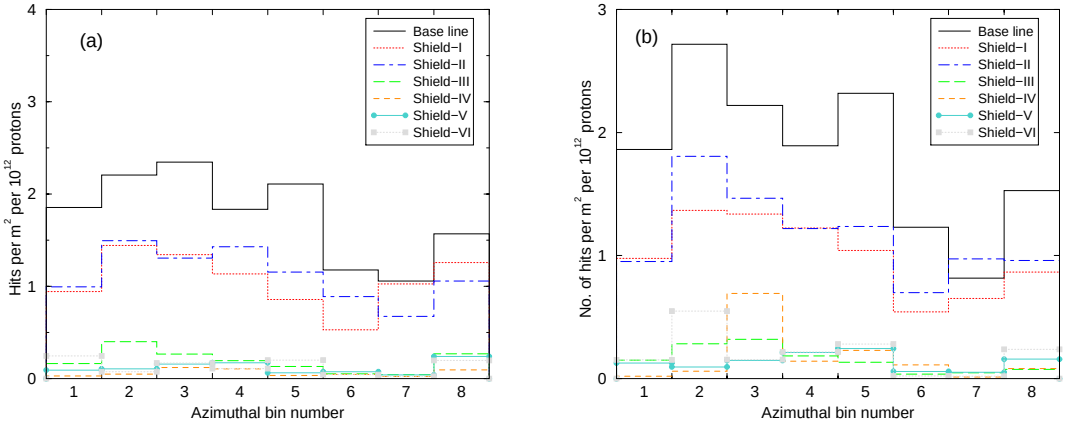

Figure 7: Azimuthal distributions of radially averaged hits in the rear plane (Run II): (a) energy deposition based calculations; (b) charged particles flux based calculations.

5 Conclusions

Installation of the combined collar shielding around the accelerator components in the hall with a 1.8-m concrete wall at the hall-tunnel interface is the most efficient way to reduce accelerator related backgrounds in the CDF forward muon system. The shielding efficiency can be as high as a factor of thirty. A slightly thicker wall at the hall-tunnel interface with a gap filled with sand bags with 10% of poly [6] (instead of pure poly) increases the shielding efficiency by another 35%.

Table 2: Total number of hits in the CDF muon spectrometer rear plane and shielding efficiency for the six shielding configurations.

Configuration	Hits	Efficiency
1	1.067	1.66
2	1.125	1.57
3	0.191	9.3
4	0.063	28
5	0.119	15
6	0.134	13

6 Acknowledgments

We express our gratitude to John Cooper, Tom Lecompte and Lee Pondrom for stimulating discussions and providing us with Run I data, and Igor Novitski for the ACAD shielding configurationy drawings.

References

[1] "The CDF II Detector TDR", Fermilab-Pub-96/390-E (1996).

[2] J. Cooper, private communication.

[3] A. I. Drozhdin, M. Huhtinen, and N. V. Mokhov, Nucl. Instruments and Methods in Physics Research, **A381**, 531 (1996).

[4] N. V. Mokhov, "Accelerator/Experiment Interface at Hadron Colliders: Energy Deposition in the IR Components and Machine Related Background to Detectors", Fermilab-Pub-94/085 (1994).

[5] N. V. Mokhov, Nuclear Physics B, **51A**, 210 (1996).

[6] J. M. Butler, D. S. Denisov, H. T. Diehl, A. I. Drozhdin, N. V. Mokhov, and D. R. Wood, "Reduction of Tevatron and Main Ring Induced Backgrounds in the DØ Detector", Fermilab-FN-629 (1995).

[7] I. Baishev, A. Drozhdin, and N. Mokhov, "STRUCT Program User's Reference Manual", SSCL-MAN-0034 (1994).

[8] N. V. Mokhov, "The MARS Code System User's Guide, Version 13(95)", Fermilab-FN-628 (1995); O. E. Krivosheev and N. V. Mokhov, "A New MARS and its Applications", Fermilab-Conf-98/043 (1998); http://www-ap.fnal.gov/MARS.

[9] L. Michelotti, "MXYZPTLK and BEAMLINE: C++ Objects for Beam Physics", in *Advanced Beam Dynamics Workshop on Effects of Errors in Accelerators, their Diagnosis and Correction*, Corpus Christi, TX, October 3-8, 1991, AIP Conf. Proceedings No. 225 (1992).

[10] L. Michelotti, "C++ Objects for Beam Physics", Proceedings of Particle Accel. Conf., San Francisco, IEEE 1991:1561-1563 (1991).